A DISSERTATION
FOR THE DEGREE OF MASTER

Cutaneous wound healing effects of mesenchymal stromal cells and sheets overexpressing platelet-derived growth factor in dogs

혈소판유래성장인자 과발현 중간엽 줄기세포와 시트의 개 피부 창상 치유 효과

by
Namyul Kim

MAJOR IN VETERINARY CLINICAL SCIENCES
DEPARTMENT OF VETERINARY MEDICINE
GRADUATE SCHOOL
SEOUL NATIONAL UNIVERSITY

August 2019

Cutaneous wound healing effects of mesenchymal stromal cells and sheets overexpressing platelet-derived growth factor in dogs

by

Namyul Kim

Supervised by
Professor Oh-Kyeong Kweon

Thesis
Submitted to the Faculty of the Graduate School
of Seoul National University
in partial fulfillment of the requirements
for the Degree of Master
in Veterinary Medicine

April 2019

Major in Veterinary Clinical Sciences
Department of Veterinary Medicine
Graduate School
Seoul National University

July 2019

Cutaneous wound healing effects of mesenchymal stromal cells and sheets overexpressing platelet-derived growth factor in dogs

혈소판유래성장인자 과발현 중간엽 줄기세포와 시트의 개 피부 창상 치유 효과

지도교수 권 오 경

이 논문을 수의학 석사 학위논문으로 제출함
2019 년 4 월

서울대학교 대학원
수의학과 임상수의학 전공
김 남 열

김남열의 석사학위논문을 인준함
2019 년 6 월

위 원 장 _____ (인)

부위원장 _____ (인)

위 원 _____ (인)

Cutaneous wound healing effects of mesenchymal stromal cells and sheets overexpressing platelet-derived growth factor in dogs

Supervisor: Professor Oh-Kyeong Kweon

Namyul Kim

Major in Veterinary Clinical Sciences

Department of Veterinary Medicine

Graduate School of Seoul National University

ABSTRACT

Adipose derived mesenchymal stem cells (Ad-MSCs) have excellent potential for use in skin repair. In addition, platelet derived growth factor (PDGF), which plays a key role at each stage of the healing process, has strong wound healing properties for normal and impaired tissues. The purpose of the present study was to compare the healing effects of PDGF-overexpressing Ad-MSCs (PDGF-MSCs) and their sheets (PDGF-CSs) with undifferentiated Ad-MSC (U-MSCs) and sheets (UCSs) on cutaneous wounds in dogs. For the *in vitro* study, all stem cells and sheets were analyzed by real-time quantitative reverse transcription polymerase chain reaction (real-time qRT-PCR). For the *in vivo* study, cells and sheets were transplanted into a square full-thickness (1.5 × 1.5 cm) skin defect model in 12 dogs, respectively.

After 5 and 10 days, wounds were harvested and evaluated macroscopically and histopathologically. The PDGF-B gene was significantly 200-fold upregulated in PDGF-CS and PDGF-MSCs groups. Upon gross analysis, all stem cells and their sheets showed accelerated cutaneous wound healing ($p < 0.05$). PDGF groups, especially PDGF-MSCs, showed significantly increased epithelialization histopathologically ($p < 0.05$). In granulation tissue, the sheets, PDGF-CSs and UCSs, promoted more upper tissue formation and deposition of collagen and activated fibroblasts than the cells, PDGF-MSCs and U-MSCs ($p < 0.05$). Especially, the PDGF-CS presented the most formation and maturation of granulation tissue. The PDGF-CS showed the most granulation tissue formation and maturation, and intradermal injection of PDGF-MSCs accelerated keratinocyte proliferation and epithelialization the most.

Key words: platelet-derived growth factor, adipose-derived mesenchymal stem cell, cell sheet, wound healing, dog

Student number: 2016-26345

CONTENTS

INTRODUCTION

Wound healing is a complex process that requires a well-orchestrated sequence, including hemostasis, cell migration, angiogenesis, extracellular matrix deposition and remodeling (Hu et al., 2014). Skin regeneration after extensive, full thickness wounding caused by burns, abrasions, or diabetic ulcers is still challenging. To accelerate skin regeneration, many tissue engineering techniques, such as the use of exogenous growth factors and cytokines, biomaterials, biocompatible scaffolds and stem cell therapy, have been investigated (Hu et al., 2014; Gowda et al., 2015; Galiano et al., 2004).

Tissue engineering using stem cells has emerged as a promising strategy for wound healing. In particular, mesenchymal stromal cells (MSCs) have excellent potential for therapeutic use in skin repair (Isakson et al., 2015). Adipose-derived mesenchymal stem cells (Ad-MSCs), a type of MSC, exhibit various advantageous properties: a large quantity of autologous cells that can easily be harvested and, the highest proliferation and differentiation potential (Kern et al., 2006). Various approaches for stem cell delivery have been attempted to increase wound healing, such as intradermal injection, cell sheets, and 3D collagen gel scaffold (Nie et al., 2011; Cerqueira et al., 2013; Kim et al., 2011). Intradermal injection around wound margins with stem cell suspensions is useful and the most commonly reported technique for wound healing using stem cells (Isakson et al., 2015). Cell sheet technology also has been a useful method for cell transplantation in regenerative medicine because high-density cell sheet constructs have the ability to increase cell residence time, have high cell survival rates, and involve no destruction of scaffolds

in transplantation sites, thus presenting more advantages than scaffold-based approaches or cell suspensions (Matsuda et al., 2007).

Platelet-derived growth factor (PDGF) is one of the growth factors that play a key role in each stage of wound healing. PDGF has been proven to proliferate granulation tissue, increase angiogenesis, and stimulate wound healing (Barrientos et al., 2008). Effects of topical application of exogenous PDGF on the acceleration of tissue repair under conditions of impaired wound healing have been demonstrated in animal models and human clinical studies (Greenhalgh et al., 1990; Embil et al., 2000; Robson et al., 2005). Human recombinant rh-PDGF-BB (Becaplermin) has been the first drug of its kind to be approved by the U.S. FDA (Food and Drug Administration) as Regranex Gel 0.01 % for use in diabetic foot ulcers in 1997, and a Phase IV clinical trial was already performed, resulting in significant increased healing and a reduction in wound closure time (Robson et al., 2005). It has been successfully applied in patients with impaired healing.

To increase the maintenance of large amounts of PDGF within the wound bed, several PDGF-gene delivery methods have been tried using the adenovirus or lentivirus in wounds (Liechty et al., 1999; Man et al., 2005), but the use of lentivirus-based PDGF-overexpressed stem cells or cell sheet therapy has not yet been reported. I hypothesized that PDGF-overexpressing Ad-MSCs (PDGF-MSCs) and their sheet (PDGF-CS) could synergize the wound healing capacities of Ad-MCSs and large quantities of PDGF secreted within the wound bed, thereby accelerating wound healing. In addition, I presumed that the wound healing response could be different depending on the cell delivery system such as sheets or cell suspensions. The purpose of the present study was to compare the effects of PDGF-CSs, PDGF-MSCs,

undifferentiated Ad-MSC sheets (UCSs) and undifferentiated Ad-MSCs (U-MSCs) in a cutaneous wound model in dogs.

MATERIALS AND METHODS

1. Isolation and culture of canine Ad-MSCs

All experimental procedures on animals in this study were approved by the Institutional Animal Care and Use Committee (IACUC) of Seoul National University in the Republic of Korea (SNU-180403-8). Canine Ad-MSCs were isolated according to a previously described procedure (Ryu et al., 2009). Briefly, adipose tissue was collected aseptically from the subcutaneous fat of the gluteal region in 2-year-old beagle dogs under anesthesia. The tissue was washed with Dulbecco's phosphate-buffered saline (DPBS; Gibco, Grand Island, NY, USA), minced, and then digested with 1 mg/ml collagenase type I (Sigma-Aldrich, USA) at 37℃ for 1 hour with intermittent shaking. The suspension was washed with DPBS and then centrifuged at 980 × *g* for 10 minutes. Stromal vascular fraction pellets were suspended with DPBS and filtered using a 100-μm nylon mesh. The samples were incubated with low-glucose Dulbecco's modified eagle medium (DMEM; HyClone, Logan, UT, USA) supplemented with 10 % fetal bovine serum (FBS; HyClone) in a humidified atmosphere at 37℃ with 5 % CO_2. The residual non-adherent red blood cells and unattached cells were removed by washing with DPBS after 24 hours. The culture medium was replaced every other day and the cells were subcultured to 80–90 % confluency. Cells were used for experimentation at the third passage.

2. Lentiviral packaging, transfection and culture of PDGF-MSCs

The canine PDGF-B gene was cloned with reference to the gene database in Pubmed. Lentiviral vector and pPACK Packaging Plasmid Mix (System Biosciences, USA) were used to clone cDNA into the vector and lentiviral packaging. According to the manufacturer's guidelines, the PDGF-B specific primer set was inserted into a pCDH-EF1-MCS-pA-PGK-copGFP-T2A-Puro vector using the restriction enzymes EcoRI and BamHI (System Biosciences, USA). HEK293T cells (Thermo Scientific) were seeded in a 100-mm dish with 10% FBS, and 1 % penicillin/streptomycin in DMEM at 37℃, 5 % CO_2. The following day, a lentiviral packaging mix (System Biosciences) and lentiviral transgene vectors were added to the cells for transfection. The cells were cultured for 48 hours at 37℃, 5 % CO_2 and the medium was changed after 15 hours. After 48 hours incubation, green fluorescent protein (GFP)-labeled PDGF-B-expressing virus particles were collected from culture media. When AD-MSCs at passage 1 reached 50–60 % confluence in the 100-mm culture dish, the PDGF-expressing virus particles were transduced into the cells. At 90 % confluence, transduced Ad-MSCs were selected using puromycin (3 μm/ml, Thermo Fisher Scientific, USA), and the culture medium was replaced after 2 days. Transduced Ad-MSCs were subcultured to 80-90 % confluence by replacing medium every 2 days, and cells at the third passage were used for experiments.

3. Cell sheet preparation: UCS, PDGF-CS

UCSs and PDGF-CSs were produced as previously described using the cell sheet fabrication method (Cerqueira et al., 2013). Ad-MSCs and PDGF-MSCs were plated at a density of 1×10^4 cells/cm^2 in a 100-mm culture dish and cultured in growth medium supplemented with 82 μg/ml L-ascorbic acid 2-phostate (Sigma, Germany) for 10 days. When cell sheets reached to 80–90 % confluence, they were retrieved by mechanical pealing with a cell scraper (SPL life science, Republic of Korea) and used for experiments.

4. Gene expression for identification of PDGF overexpression using real-time qRT-PCR

Total RNA was isolated using a Hybrid-RTM RNA extraction kit (GeneAll Biotechnology, Republic of Korea) and the RNA concentration was measured with an Epoch microplate spectrophotometer (BioTek Instruments, Inc., USA). Complementary DNA (cDNA) was synthesized using a PrimeScript II First-strand cDNA Synthesis Kit (Takara Bio Inc., Japan) according to the manufacturer's protocol. Real-time quantitative reverse transcription polymerase chain reaction (real-time qRT-PCR) was performed using an StepOnePlus™ Real-Time PCR system (Thermo Fisher Scientific, USA) with SYBR® Premix Ex Taq™ (Takara Bio Inc., Japan). Expression levels of each target gene were normalized to those of glyceraldehyde 3-phosphate dehydrogenase (GAPDH) using the ΔΔCT method.[17] Primer sequences for target genes are listed in Table 1.

Table 1. Primers for quantitative real-time polymerase chain reaction

Gene		Primer sequence (5'–3')
PDGF-B	**Forward**	CCGAGGAGCTCTACGAGATG
	Reverse	AACTCTCCAGCTCGTCTCCA
VEGF	**Forward**	CTATGGCAGGAGGAGAGCAC
	Reverse	GCTGCAGGAAACTCATCTCC
COX-2	**Forward**	ACCCGCCATTATCCTAATCC
	Reverse	TCGGAGTTCTCCTGGCTTTA
IL-6	**Forward**	TTTTCTGCCAGTGCCTCTTT
	Reverse	GGCTACTGCTTTCCCTACCC
IL-10	**Forward**	CCTGGGAGAGAAGCTCAAGA
	Reverse	TGTTCTCCAGCACGTTTCAG
TNF-α	**Forward**	ACCACACTCTTCTGCCTGCT
	Reverse	TGGAGCTGACAGACAACCAG
KGF	**Forward**	AGCCCTGAGCGACATACAAG
	Reverse	TGCCACTATTCCAACTGCCA
EGF	**Forward**	TGTGTCTGGCTCTGAATGGC
	Reverse	AAGACATCCCCTGGCGTTAC
IGF-1	**Forward**	AAATCAGCAGTCTTCCAACCCA
	Reverse	ACACGAACTGAAGAGCGTCC
FGF-2	**Forward**	TGCCTACCTAGATGCTGGACA
	Reverse	GAGCTTTGGCCGTATTTCCATTC
GAPDH	**Forward**	CATTGCCCTCAATGACCACT
	Reverse	TCCTTGGAGGCCATGTAGAC

PDGF-B, platelet-derived growth factor B; VEGF, vascular endothelial growth factor; COX-2, cyclooxygenase-2; IL-6, interleukin-6; IL-10, interleukin-10; TNF-α, tumor necrosis factor-α; KGF, keratinocyte growth factor; EGF, epidermal growth factor; FGF-2, fibroblast growth factor 2; IGF-1, insulin-like growth factor-1; GAPDH, glyceraldehyde-3-phosphate dehydrogenase

5. Transplantation into full-thickness excisional wound models

Animals

Twelve healthy adult beagle dogs (2–3 years old, 10.1 ± 1.8 kg) were studied. All dogs were cared for accordance with the animal care guidelines of the Institute of Laboratory Animal Resources in Seoul National University. All animals were considered to be healthy based on physical examination, complete blood count, and serum chemistry. Animals were caged individually under a standard environment.

Anesthesia

Animals were pre-medicated with medetomidine (5 μm/kg, intravenously [IV]), tramadol (4 mg/kg, IV) and cefazolin (22 mg/kg, IV). Anesthesia was induced with alfaxalone (2 mg/kg, IV) and maintained with isoflurane 1.5 % with oxygen. Lactated Ringer's solution was administered via IV at 10 mg/kg/h. Heart rate, blood pressure, respiratory rate, rectal temperature, end tidal CO_2, pulse oximetry and spirometer were checked with an anesthetic monitoring system (GE healthcare, USA) throughout anesthesia. Each animal was positioned in sternal recumbency, and the dorsal area from the cranial part of the thorax to the middle part of abdomen was clipped and prepared aseptically.

Wound creation and transplantation of stem cells and their sheets

All animal experimental protocols were approved by the Institutional Animal Care and Use Committee (IACUC) of Seoul National University in the Republic of Korea (SNU-180403-8) and all surgical procedures were performed with respect to international animal welfare rules. Six full-thickness wounds were created

with a #15 scalpel blade on either side of the dorsal region. Each wound size was 1.5 × 1.5 cm and each wound on a side was separated by 3 cm as not to interrupt other wounds during healing (Figure 1). Wounds were randomly assigned into six groups: PDGF-CS, UCS, PDGF-MSCs, U-MSCs and control groups for sheets (Control-S) and cells (Control-M). In PDGF-CS or UCS groups, the cell sheets were carefully placed and covered the entire wound beds. In PDGF-MSC or U-MCS groups, 1-ml cell suspensions were injected with 1 ml syringe and 26-G needle intradermally around the wound area. In the Control-S groups, wounds were not treated with anything, and in the Control-M groups, 1 ml saline was injected in the same way as described for the cell groups. Wounds were covered with sterile adhesive dressing (Hiper-pore®, WON Biogen, Republic of Korea) and cotton rolls (Daehan medical, Republic of Korea) were applied in multiple layers with crossing over the shoulders and between forelimbs to prevent the bandage from slipping caudally. Lastly, an elastic bandage (Daehan medical, Republic of Korea) as a tertiary layer was applied over the cotton roll layers.

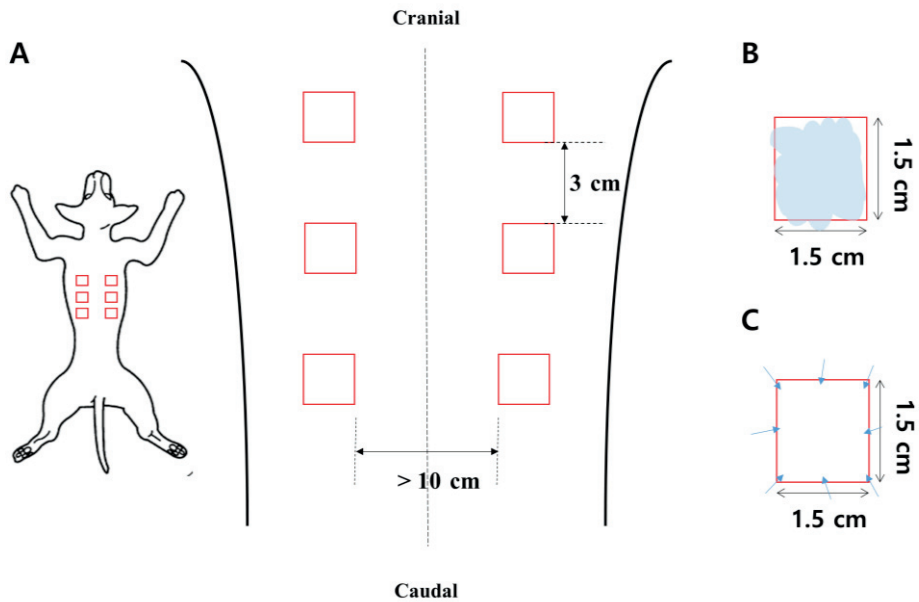

Figure 1. Wound creation and transplantation of a stem cell sheet and a stem cell suspension into the wound. (A) The layout of full-thickness wounds created on the dorsal region in the dog. The wounds were made bilaterally and the size of the wounds was 1.5 × 1.5 cm (square). Wounds were 3 cm away from each other. (B) In sheet groups (PDGF-CS and UCS), a cell sheet was placed to cover the entire wound area and (C) in cell groups (PDGF-MSCs and U-MSCs), a cell suspension was injected intradermally at eight injection sites around the wound edge.

6. Evaluation of wound healing

Gross analysis

Digital photographs of wounds were taken at days 5 and 10. Percentages of epithelialization, contraction, and total wound healing were measured as previously described (Bohling et al., 2004) using Image J software (Wayne Rasband, NIH, USA). Briefly, the most outer margin area of the wound was considered as the total wound area (A), the area within the outer margin of the unhealed wound was the open wound area (B) and the area between these two margins was the area of epithelialization (C). Within these areas, the percent of epithelialization, contraction and total wound healing were calculated as follows (Figure 2).

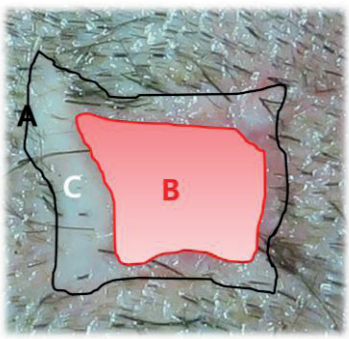

$$\% \text{ epithelialization} = \frac{\text{Area of epithelium}}{\text{Total wound area}} \times 100$$

$$\% \text{ contraction} = 100 - \frac{\text{Total wound area}}{\text{Original wound area}} \times 100$$

$$\% \text{ total wound healing} = 100 - \frac{\text{Open wound area}}{\text{Original wound area}} \times 100$$

Figure 2. Scheme of wound area and the calculation method of the percent of epithelialization, contraction and total wound healing. A. Total wound area: the area within the outer line between the normal skin and epithelium of the wound is the total wound area. B. Open wound area: the area within the outer margin between the open wound and wound epithelium is the open wound area. C. Area of epithelium: the area of advancing of the newly formed epithelium is the area of epithelium.

Histopathological Analysis

Skin samples including wounded and adjacent normal skin were harvested at days 5 and 10, fixed in 10 % formalin for 24 hours, and embedded in paraffin. H&E and Masson's trichrome staining were conducted using routine protocols. All samples were scanned by a microscope slide scanner (Pannoramic® SCAN II, 3D HISTECH Ltd., Hungary) and analyzed in a blinded fashion using a slide images analysis program (CaseViewer™, 3D HISTECH Ltd., Hungary).

Thickness and shape of neo-epidermis: On H&E-stained samples, the shape and thickness of the neo-epidermis overlying the wound edge was evaluated based on the previously described method (Larouche et al., 2011). Briefly, 10 parts of randomly selected neo-epidermis were measured in each tissue section and compared among groups at days 5 and 10, respectively.

Quantification and maturation of granulation tissue: The quantity and quality of newly formed granulation tissue in H&E-stained samples were assessed, respectively, by measuring granulation tissue size of the wound bed between unwounded skins and calculating the histological score index (HS index, HS/mm^2), an average of the histological score per granulation tissue, based on a histological score (HS) that ranges from 1 to 12 (Table 2) (Jacobi et al., 2002). Granulation tissues at day 10 were divided into upper and lower layers and calculated; upper granulation tissue is rich in inflammatory cells and vessels and lower granulation tissue is rich in collagens and connective tissues. Calculation of the HS index was performed as follows.

Table 2. Histological scoring system

Scores	Granulation tissue
1-3	None to minimal cell accumulation, no granulation tissue or epithelial travel
4-6	Thin, immature granulation, dominated by inflammatory cells with a few fibroblasts, capillaries, or collagen deposition, and minimal epithelial migration
7-9	Moderately thick granulation tissue, dominant inflammatory cells, more fibroblasts and collagen deposition, extensive neovascularization, and minimal to moderate migrating epithelium
10-12	Thick, vascular granulation tissue dominated by fibroblasts and extensive collagen deposition, and epithelium partially to completely covering the wound

Quantification of vessels density: The number of blood vessels was quantified at days 5 and 10 in H&E-stained samples. In 10 randomly selected 100× magnification fields, all visible blood vessels within the fields were counted and the mean number of vessels per the fields was calculated. The number of vessels was normalized to the tissue area. Blood vessels were defined as vascular structures based on typical morphological appearance and well-defined vascular lumen and intraluminal red blood cells.

***Collagen abundance and organization*:** In Masson's trichrome-stained slides, collagen abundance and organization were evaluated by modifying the scale from 0–11 (Farghali et al., 2017). Briefly, the scoring was as followes: 0–2, no to rare collagen or disorganized collagen fibers in granulation tissues; 3–5, mild collagen deposition that comprised 25–50% of granulation tissues and randomly orientated collagen fibers; 6–8, moderate collagen deposition that comprised 50–75% of granulation tissues, and well-oriented collagen fibers. 9–11, abundant total collagen that comprised most of the granulation tissues and well-organized fibers. Parallel-oriented wavy collagen fibers with well-stained blue color were considered to be more organized than randomly disorientated and inconsistent blue-colored collagen fibers.

Immunohistochemical analysis

To identify keratinocytes proliferation in the neoepidermis and activated fibroblasts in the granulation tissues, immunohistochemistry was performed with primary antibodies against Ki67(rabbit polyclonal IgG, ab155580, 1:1000, Abcam Cambridge, MA) as a proliferation marker and fibroblast activation protein, alpha

(FAP) (rabbit polyclonal IgG, ab53066, 1:100, Abcam Cambridge, MA) as reactive fibroblasts marker. Briefly, 5 μm frozen paraffin sections were deparaffinized and rehydrated, and the heat-induced antigen retrieval method was conducted using a pressure cooker in 10mM citrate buffer solution. Endogenous enzymes were inactivated with 0.3% H_2O_2 for 30 min and nonspecific antibody binding was blocked with 2.5 % normal serum blocking solution (S-1012, Vector labs, CA). The sections were incubated overnight at 4℃ with primary antibodies, then incubated with anti-rabbit IgG biotinylated secondary antibody(ImmPRESS^{TM} HRP reagent kit, Vector labs, CA) for 30 min at room temperature, followed by 3,3`-diaminobenzidine (DAB; Vector labs) for 2 min. Lastly, counterstain was performed with hematoxylin and sections were mounted and examined under a light microscope.

The number of Ki67-positive cells in the neoepidermis was counted in 10 randomly selected 400× magnification fields, and the mean number of expressed cells per the fields was calculated. Nuclei stained to brown or claybank was considered a positive cell. For quantification of FAP, 10 random fields per granulation tissue at 200× magnification were chosen, and a semiquantitative scale of 1 to 8 was used. The rating scale is described as follows: 1–2, rare to minimum fibroblasts stained in granulation tissue; 3–4, mild and irregular pattern of activated fibroblasts; 5–6, moderate and well-oriented fibroblasts over granulation tissue; 7–8, abundant, dense and compact organized fibroblasts all over the granulation tissue.

7. Statistical analysis

The values are presented as the means ± standard deviation (SD). All statistical analyses were performed using the IBM SPSS statistics 23.0 software (Chicago, IL, USA). Data analysis was carried out by the Kruskal-Wallis test with Mann-Whitney's post hoc test. A p value of less than 0.05 was considered statistically significant.

RESULTS

1. Morphology and gene markers expression of cells and their sheets

PDGF-MSCs and U-MSCs had similar morphology, and via microscopy and gross observation of a condensed contiguous layer, it was confirmed that their sheets were successfully made (Fig 3A(a)). Also, through GFP expression under fluorescence microscopy, it was confirmed that PDGF-MSCs were successfully transfected with PDGF-B (Fig 3A(b)). Of the gene markers, PDGF-B was upregulated by approximately 200-fold in PDGF-CSs and PDGF-MSCs, which was the most remarkable upregulation among the genes (Figure 3B(a)). The VEGF gene, a vascular related marker, was approximately 1.5-fold upregulated in PDGF-CS and PDGF-MSCs ($^{+}p < 0.05$) (Figure 3B(b)) and COX-2 and IL-6, inflammatory markers, were also approximately 2-fold upregulated in those groups ($^{+}p < 0.05$) (Figure 3B(c), (d)). The FGF-2 gene was more upregulated in the sheet groups ($^{*}p < 0.05$) (Figure 3j). Epidermis markers, KGF, EGF, and IGF-1, were not significantly expressed in any of the groups (Figure 3B(g), (h), (i)). IL-10 and TNF-α also were not noticeably expressed among the groups (Figure 3B(e), (f)).

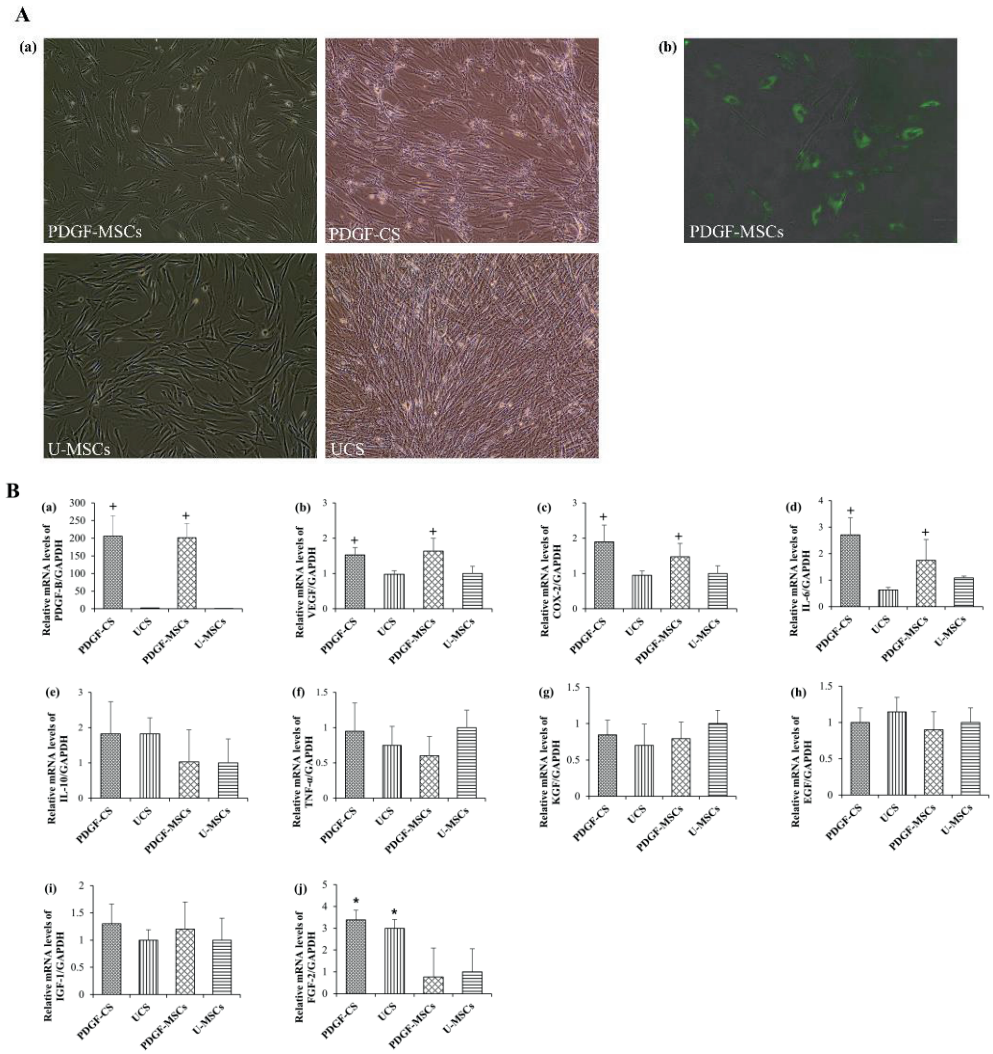

Figure 3. Microscopic/fluorescence images and gene expression in PDGF-CSs, UCSs, PDGF-MSCs and U-MSCs. A. (a) Morphology of cells and their sheets under microscopy (200×). (b) The fluorescence expression of GFP in PDGF-MSCs depicting the successful transfection of PDGF genes (400×). B. The mRNA expression of PDGF-B, VEGF, COX-2, and IL-6 was significantly more upregulated in PDGF-CSs and PDGF-MSCs than in UCSs and U-MSCs ($^{+}p < 0.05$), and that of FGF-2 was more upregulated in the sheet groups than in the cell groups ($^{*}p < 0.05$). The PDGF-B gene upregulation was the most significant among genes ($^{+}p < 0.05$)

and for IL-10 and TNF-α gene expression, no statistically significant difference was observed among groups. Also, the genes of epidermis markers, KGF, EGF, and IGF-1, were not significantly expressed in any groups. $^{+}p < 0.05$ versus undifferentiated groups (UCS, U-MSCs), $^{*}p < 0.05$ versus cell groups.

2. Gross findings in wounds

Percent epithelialization

At day 5, mean percent epithelialization in all stem cell and sheet groups was significantly greater than in the control groups ($^{\#}p < 0.05$, $^{\#\#}p < 0.01$). The PDGF-MSCs group showed a higher epithelialization rate as compared to undifferentiated groups like UCS and U-MSCs groups ($^{+}p < 0.05$) (Figure 4B). As shown in the day 5 gross images, the PDGF-MSCs groups presented wider and thicker epithelialization than other groups (Figure 4A). At day 10, a similar pattern was identified; all stem cell and sheet groups showed higher epithelialization than control groups ($^{\#}p < 0.05$, $^{\#\#}p < 0.01$) and PDGF-CS and PDGF-MSCs groups tended to have higher rates than UCS and U-MSCs groups, although this was not significant (Figure 4C, D).

Percent contraction

Mean percent contraction on day 5 for stem cell groups (PDGF-MSCs, U-MSCs) and sheet groups (PDGF-CS, UCS) seemed to be higher than that for all control groups, but not statistically different (Figure 4B). At day 10, stem cell groups ($^{\#\#}p < 0.05$) and sheet groups ($^{\#\#}p < 0.01$) had a significantly higher contraction rate than control groups (Figure 4D). However, no significant difference was observed among experimental groups at days 5 and 10 (Figure 4A-D).

Percent total wound healing

At both days 5 and 10, the total wound healing rate of stem cell groups ($^{\#\#}p < 0.05$) and sheet groups ($^{\#\#}p < 0.01$) was significantly higher than that of the control groups (Figure 4B, D). No statistically significant difference regarding total wound healing was observed among experimental groups at days 5 and 10 (Figure 4B, D).

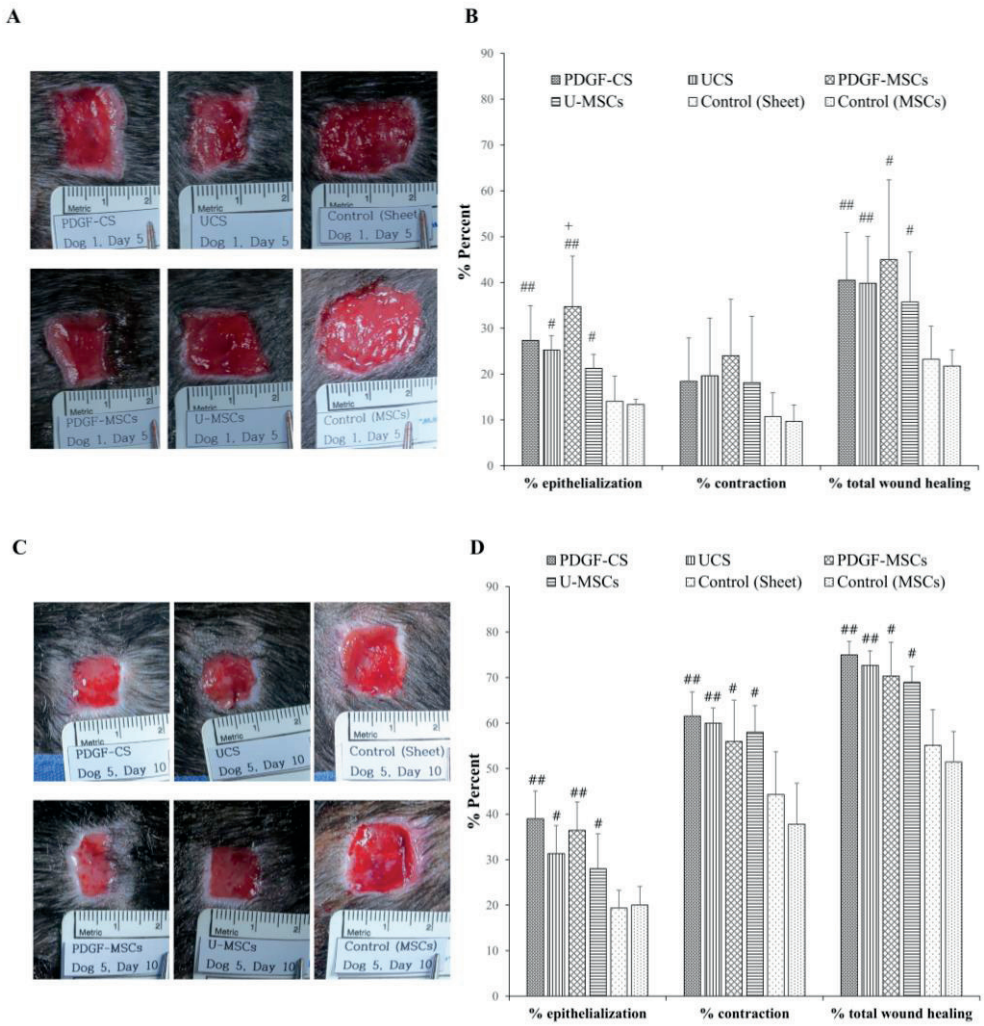

Figure 4. Gross images of wound healing and evaluation of epithelialization, contraction, and total wound healing rates at days 5 and 10. Representative macroscopic images of experimental groups and control groups at days 5 (A) and 10 (C). Percent of epithelialization, contraction, and total wound healing was calculated using photographs of wounds at days 5 (B) and 10 (D); $^{\#}p < 0.05$ and $^{\#\#}p < 0.01$ versus the control groups, $^{+}p < 0.05$ versus undifferentiated groups (UCS, U-MSCs).

3. Granulation tissue formation and maturation in wounds

The absolute amount of newly formed granulation tissue was not significantly different among groups at day 5 (Figure 5C). However, the shape of granulation tissue among groups was significantly different. The width and depth of granulation tissues in sheet and cell groups were shorter and deeper than those in control groups (Figure 5A). The granulation tissue of sheet and cell groups seemed to be denser and more compact, especially PDGF-CS and UCS groups. The histological score index of PDGF-CS and UCS groups was significantly higher than that of control groups ($^{\#}p < 0.05$) (Figure 5B, D). PDGF-MSCs and U-MSCs groups also showed higher infiltration of inflammatory cells and fibroblasts than control groups, but this was not significant.

At day 10, the size and depth of granulation tissues of PDGF-CS and UCS groups were more prominent (Figure 6A). The amount of upper granulation tissue in PDGF-CS and UCS groups ($^{\#}p < 0.05$, $^{*}p < 0.05$) was significantly greater than that in cells and control groups. Lower granulation tissues sizes in sheet ($^{\#\#}p < 0.01$) and cell groups ($^{\#}p < 0.05$) were significantly greater than in control groups, and the total granulation tissues in the sheet ($^{\#\#}p < 0.01$) and cell groups ($^{\#}p < 0.05$) were significantly more organized than in control groups (Figure 6A, B). Among experimental groups, the PDGF-CS groups presented the largest granulation tissue size and when compared to cell groups, significantly greater tissue sizes were observed ($^{*}p < 0.05$) (Figure 6B).

In the assessment of tissue maturation at day 10 using the HS index, upper granulation tissues in sheet and cell groups showed a higher density of fibroblasts, blood vessels and collagen deposition than in control groups ($^{\#}p < 0.05$, $^{\#\#}p < 0.01$)

(Figure 6C, D). Especially the upper granulation of PDGF-CS groups showed the most monocytes infiltration, large diameter of blood vessels and the highest density of fibroblasts, and collagen that smoothly connected to lower granulation tissues ($^{=}p < 0.05$). Lower granulation tissues presented high maturation of tissue conditions dominated by extensive collagens, fibroblasts, and no PMNL in all the groups (Figure 6C, D). Overall, the quality of total granulation tissues in sheets ($^{\#\#}p < 0.01$) and cell groups ($^{\#}p < 0.05$) was higher than in control groups and PDGF-CS had the highest histological score on upper granulation tissue and total granulation tissue among groups ($^{\#\#}p < 0.01$, $^{=}p < 0.05$) (Figure 6C, D).

4. Vascular density

At day 5, the density of blood vessels in the granulation tissue was not significantly different among the groups. At day 10, the number of blood vessels increased and a significant difference was found. PDGF-CS, PDGF-MSCs, UCS groups ($^{\#\#}p < 0.01$) and the U-MSCs group ($^{\#}p < 0.05$) showed more blood vessels in the wound tissues than the control groups (Figure 6C, E). Despite no statistical difference among experimental groups, PDGF-CS and PDGF-MSCs groups presented a tendency to have large diameter vessels, as well as the most and the second most number of blood vessels among the groups (Figure 6C, E).

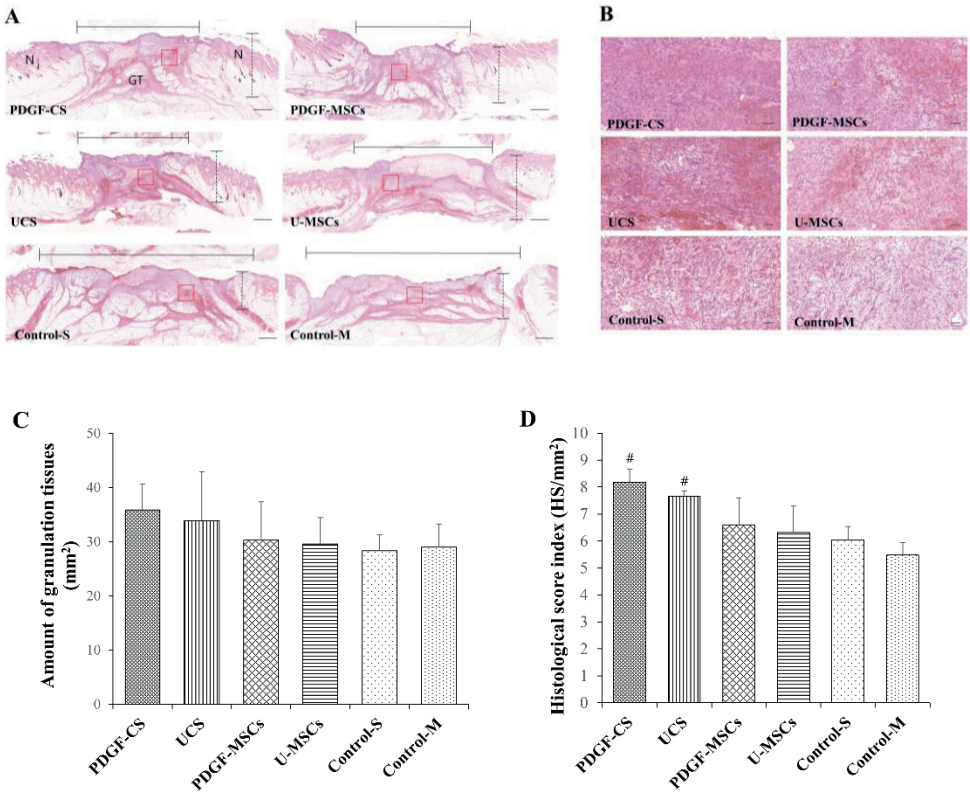

Figure 5. Histological analysis for quantification and maturation of granulation tissues in wounds at day 5. (A) Representatives image of entire wound area with adjacent normal skin stained with H&E (8×, scale bar 1000 μm). Horizontal full lines indicate the width of granulation tissue between wound margins and vertical dotted lines indicate the depth of new granulation tissue in the wound area. (B) Representatives image of magnifying the granulation tissues (red square in A). (200×, scale bar 50 μm). (C) Representation of the amount of granulation tissue and (D) histological score index in wound area. GT, granulation tissue; N, normal skin; $^{\#}p <$ 0.05 versus the control groups

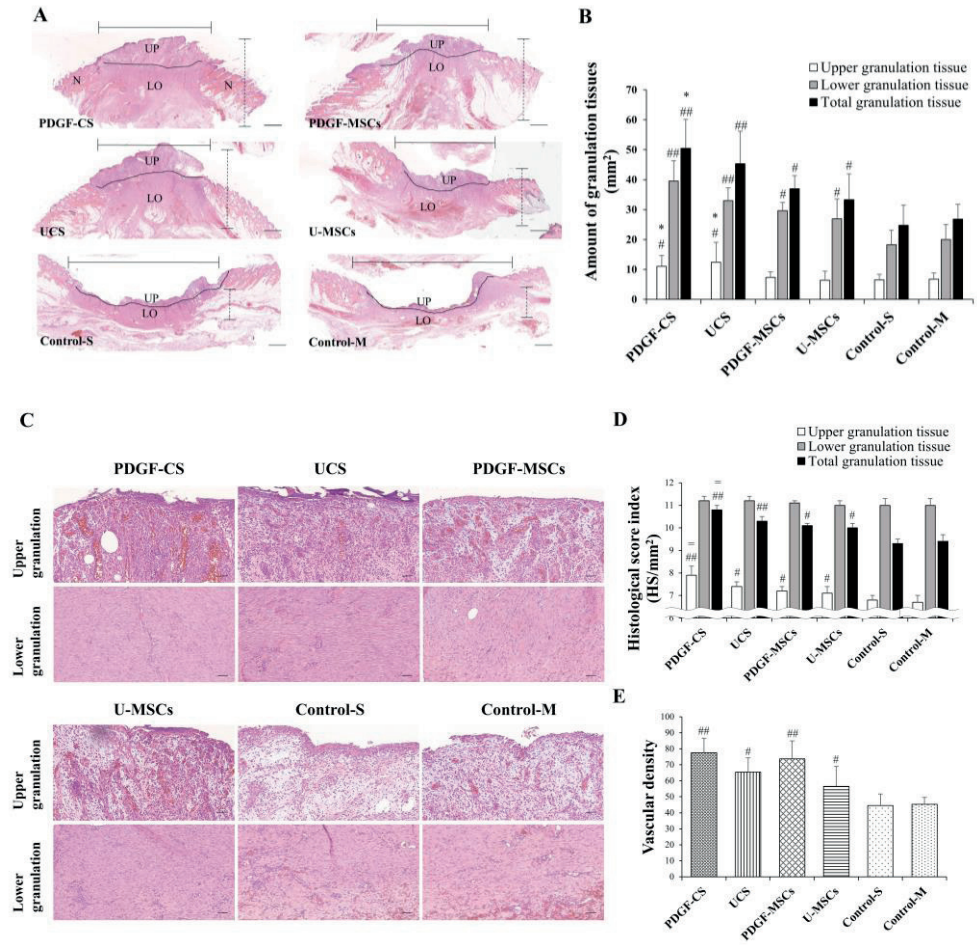

Figure 6. Histological analysis for quantification and maturation of granulation tissues in wounds at day 10. (A) Representatives image of entire wound area with adjacent normal skin with H&E stain (8×, scale bar 1000 μm). Horizontal straight lines above tissues indicate the width of granulation tissue and vertical dotted lines indicate the depth of new granulation tissues in the wound area. Upper and lower granulation tissues are distinguished by a curved line. (B) Representation of the amount of upper, lower, and total granulation tissues. (C) Representatives image of magnifying the upper granulation tissue (100×, scale bar 100 μm) and lower granulation tissue (200×, scale bar 50 μm) with H&E stain. Representation of

histological score index (D) and vascular density (arrow: blood vessel) (E) in wound area. UP, upper granulation tissue; LO, lower granulation tissue; N, normal skin; $^{\#}p < 0.05$, $^{\#\#}p < 0.01$ versus the control groups, $^{*}p < 0.05$ versus cell groups, $^{=}p < 0.05$ versus the rest of the groups

5. Collagen deposition

At day 5, collagen deposition in wounds of sheet groups ($^{\#\#}p < 0.01$, $^{*}p < 0.05$) significantly increased when compared to both control and cell groups (Figure 7A, B). Collagen in the wounds of the control groups was rarely found and wounds in the cell groups showed more collagen fibers than in control groups, but this was not significant (Figure 7A, B). At day 10, wounds in all sheet ($^{\#\#}p < 0.01$) and cell groups ($^{\#}p < 0.05$) had significantly more collagen infiltration than in control groups and PDGF-CS groups ($^{=}p < 0.05$) showed significant collagen deposition and much denser and thicker fibers in wounds than the rest of the groups (Figure 7C, D).

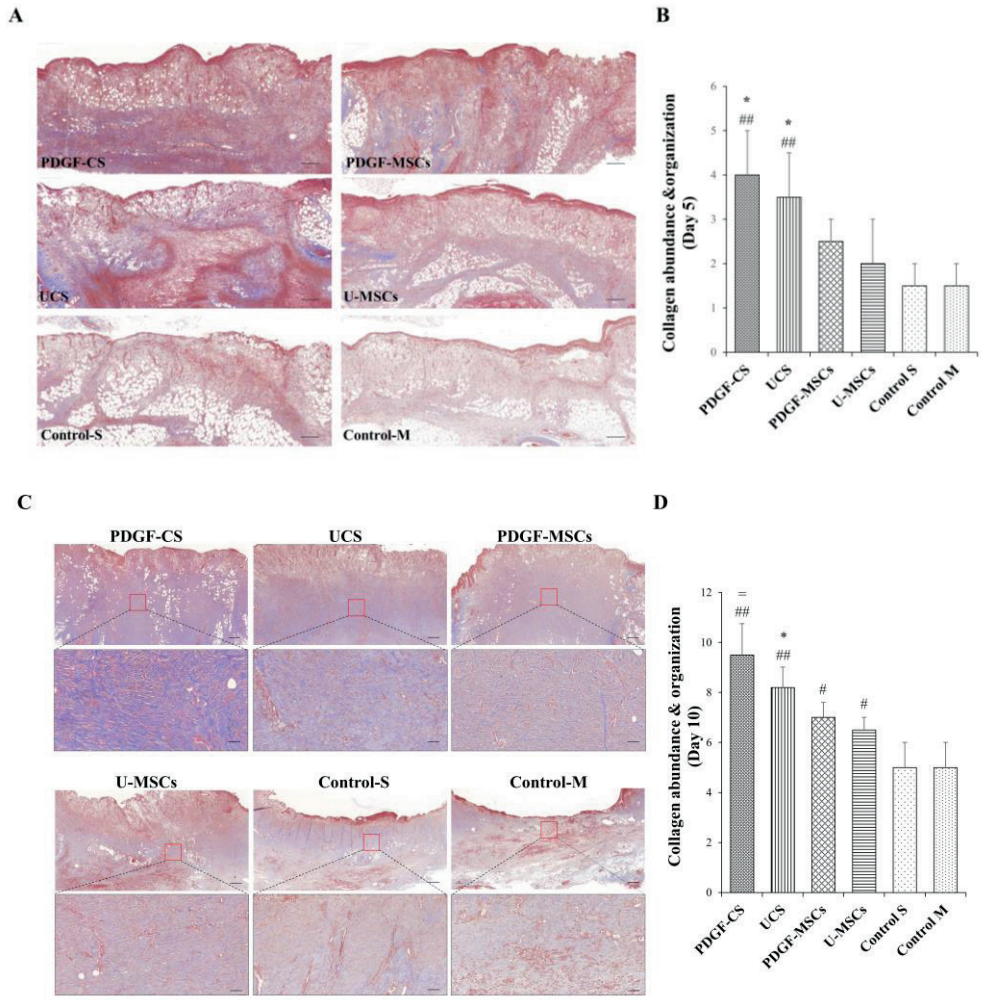

Figure 7. Collagen deposition and organization in wounds. (A) Representative images of collagen deposition in wounds at day 5 (Masson's trichrome, 30×, scale bar 500 μm). (B) Quantitative data of collagen abundance and organization at day 5. (C) Representative images of collagen deposition in wounds at day 10 (Masson's trichrome, 25×, scale bar 500 μm) and inset high magnification images indicated collagen density and collagen fibers orientation (200×, scale bar 50 μm). (D) Quantitative data of collagen abundance and organization at day 10. $^{\#}p < 0.05$, $^{\#\#}p <$

0.01 versus the control groups, $^{*}p < 0.05$ versus cell groups, $^{=}p < 0.05$ versus the rest of the groups.

6. Epithelialization

From histological observation of H&E images, it was clear that the shape and the thickness of the neoepidermis were different among groups. First, PDGF groups like PDGF-CS and PDGF-MSCs groups ($^{\#\#}p < 0.01$) and undifferentiated groups like UCS and U-MSCs groups ($^{\#}p < 0.05$) showed a longer and thicker neoepidermis than that in control groups both at days 5 and 10 (Fig 8A, B). While the epidermis in the control groups was hypertrophied and migrated a little over the granulation tissue adjacent to the normal tissue (Fig 8A(e), (e'), (f), (f')), the epidermis in the experimental groups was greatly hypertrophied and actively migrated and invaded over the granulation tissue (Fig 8A(a)(a') – (d)(d')) at days 5 and 10. Among the experimental groups, only PDGF-MSCs groups at day 5 and PDGF-MSCs and PDGF-CS groups at day 10 presented prominent rete ridges-like structures (Fig 8A; dashed lines under neoepdermis) and skin appendages like hair follicles frequently (Fig 6A; arrow head). Moreover, those PDGF groups showed a significant difference regarding the shape and thickness of neoepidermis when compared to undifferentiated groups ($^{+}p < 0.05$, $^{++}p < 0.01$) (Fig 8A(a'), (c), (c'), B). The PDGF-MSCs groups showed the thickest neoepidermis among groups at both days 5 and 10.

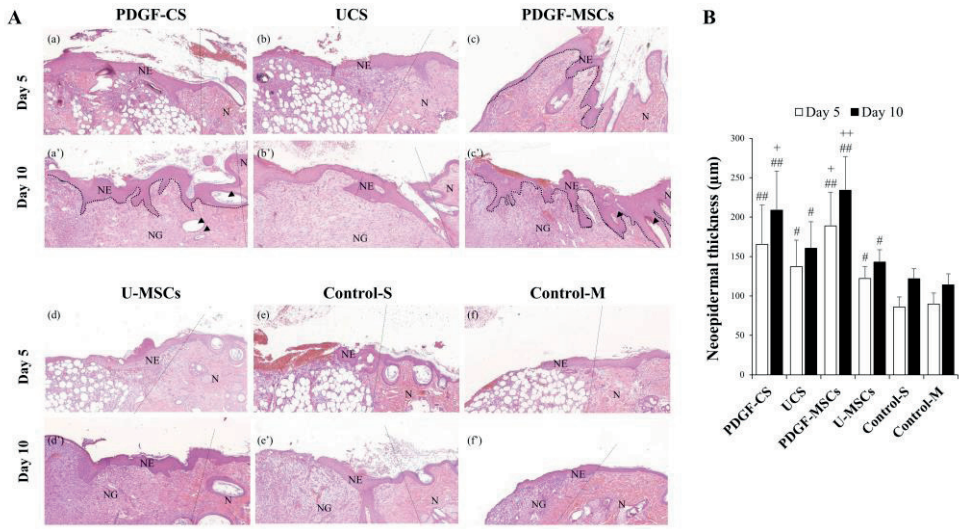

Figure 8. Neoepidermis shape and thickness measurement. (A) Representative images of epidermis regeneration at day 5 (a – f) and day 10 (a' – f') stained with H&E (80×) evidencing the difference in the shape and thickness of the neoepidermis among groups. Rete ridges-like structures (outlined by the dashed line) were identified in the neoepidermis of PDGF-MSCs groups (c) at day 5 and PDGF-CS (a') and PDGF-MSCs (c') groups at day 10. The regeneration of the skin appendages such as hair follicle (arrow head) was identified in the neoepidermis and neogranulation of PDGF-CS (a') and PDGF-MSCs (c') groups at day 10. A straight dotted line indicates the border between a wound and normal skin. (B) Quantitative data of neoepidermis thickness at days 5 and 10. NE, neoepidermis; NG, neogranulation; N, normal skin; $^{\#}p < 0.05$, $^{\#\#}p < 0.01$ versus the control groups, $^{+}p < 0.05$, $^{++}p < 0.01$ versus undifferentiated groups (UCS, U-MSCs).

7. Keratinocyte proliferation

At day 5, in the control groups, Ki67 expression was identified mostly in basal layers (Fig 9A(e),(f)), while for experimental groups, its expression was found in both basal and suprabasal layers (Fig 9A(a) – (d)) and especially in PDGF-MSCs groups, the expression was distinct (Fig 9A(c)). Moreover, at day 10, its expression was located within most of the basal cells and several suprabasal cells in the control groups (Fig 9A(e'),(f')), while in experimental groups, the expression was found throughout the basal and suprabasal layers (Fig 9A(a) – (d)). Rete ridge-like structures in the PDGF-MSCs groups showed the most prominent Ki67 expression throughout the layers among groups (Fig 9A(c')).

The number of Ki67 expressing cells in the neoepidermis also differed among groups (Fig 9B). All experimental groups had more expression cells than the control groups at days 5 and 10 ($^{\#}p < 0.05$, $^{\#\#}p < 0.01$). At day 5, only the PDGF-MSCs groups and at day 10, PDGF-CS and PDGF-MSCs groups presented significantly more Ki67 expression when compared to undifferentiated groups such as UCS, U-MSCs groups ($^{+}p < 0.05$, $^{++}p < 0.01$). The PDGF-MSCs groups showed the greatest number of expression cells among experimental groups at days 5 and 10 (Fig 9B).

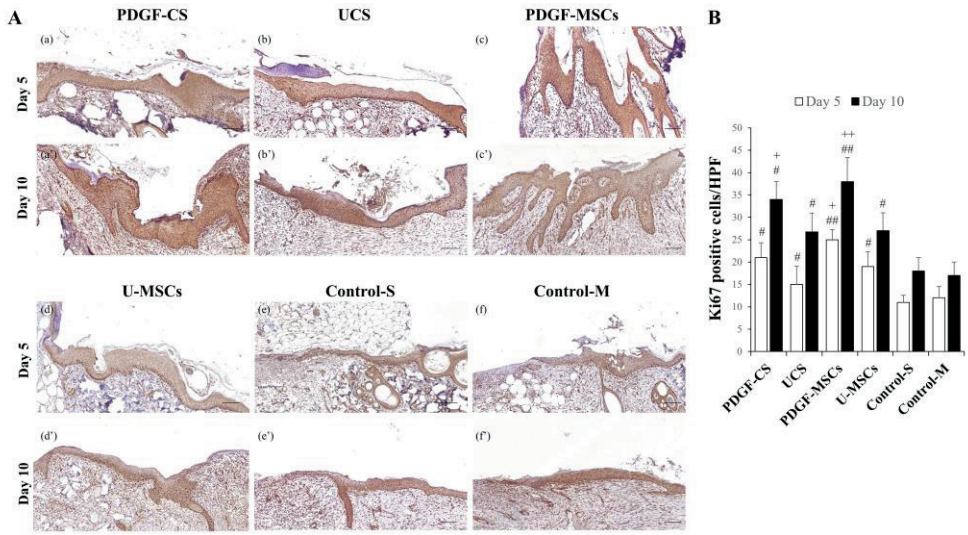

Figure 9. Keratinocyte proliferation (Ki67) in the neoepidermis. (A) Immunohistochemical analysis of the expression of Ki67 in the epidermis at day 5 (a – f) and day 10 (a' – f') (120×, scale bar 100 μm) evidencing the different pattern and number of its expression in neoepidermis among groups. (B) Quantitative data of Ki67-positive cells of the neoepidermis in the high power field (400×) at days 5 and 10. $^{\#}p < 0.05$, $^{\#\#}p < 0.01$ versus the control groups, $^{+}p < 0.05$, $^{++}p < 0.01$ versus undifferentiated groups (UCS, U-MSCs).

8. Activated stromal fibroblasts

Activated stromal fibroblasts were similarly presented as collagen depositions. At day 5, PDGF-CS (5.0 ± 0.7) and UCS (4.5 ± 0.8) groups indicated significantly higher expression than control-S (2.5 ± 0.5) and control-M (2.25 ± 0.4) groups ($^{\#}p < 0.05$) and the PDGF-CS group (5.0 ± 0.7) (Figure 10(a)) showed the most FAP expression (Figure 10(a), (b), (e), (f)). At day 10, PDGF-CS groups (7.25 ± 0.4) (Figure 10(a')) had the most well-oriented, abundant and densely expressed fibroblasts among groups and showed more significantly expressed stains than the rest of the groups ($^{\#\#}p < 0.01$, $^{=}p < 0.05$) (Figure 10(a') – (f')). The UCS (6.75 ± 0.4) groups indicated more FAP expression than cell groups ($^{\#\#}p < 0.01$, $^{*}p < 0.05$). PDGF-MSCs (5.25 ± 0.4) (Figure 10(c')) and U-MSCs (5.5 ± 0.5) (Figure 10(d')) groups presented significant expression compared to control-S (3.5 ± 0.5) (Figure 10(e')) and control-M (3.75 ± 0.4) (Figure 10(f')) ($^{\#}p < 0.05$). No statistical difference between PDGF-MSCs and U-MSCs was observed at days 5 and 10.

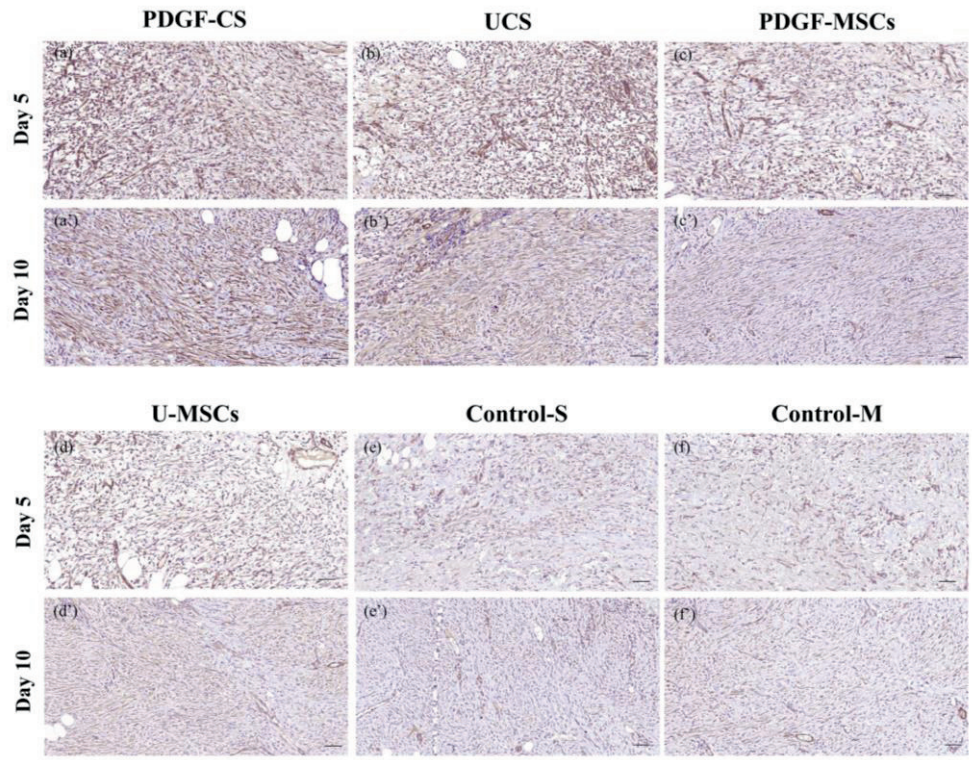

Figure 10. Activated stromal fibroblasts in granulation tissues (fibroblast activation protein alpha (FAP)). Immunohistochemical analysis of the expression of FAP in granulation tissues at day 5 (a – f) and day 10 (a' – f') (200×, scale bar 50 μm) evidencing the different density and pattern of its expression among groups. $^{\#}p < 0.05$, $^{\#\#}p < 0.01$ versus the control groups, $^{*}p < 0.05$ versus cell groups, $^{=}p < 0.05$ versus the rest of the groups.

DISCUSSION

In the present study, our results showed that all experimental groups, irrespective of cell delivery method and PDGF overexpression, PDGF-CS, UCS, PDGF-MSCs, and U-MSCs, accelerated cutaneous wound healing. Among them, PDGF groups, especially PDGF-MSCs, significantly increase epithelialization histopathologically. The sheets (PDGF-CS and UCS) covering wound beds engaged in more of a granulation tissue response than cells (PDGF-MSCs and U-MSCs) injecting intradermally around wound margins. Among the sheets, PDGF-CS enhanced the maturation of granulation tissues the most.

MSCs have been used to improve wound healing under impaired or normal condition (Isakson et al., 2015). The mechanism of action is not fully understood; however two main mechanisms are noted: releasing paracrine factors for wound healing like key cytokines, growth factors (PDGF, VEGF), and inflammatory mediators (TNF-α, IL-6) and cells themselves participating in the healing process, ultimately differentiating into skin structures (Isakson et al., 2015). Among paracrine factors, PDGF, a potent growth factor that is FDA approved for wound healing, has been proven to enhance the proliferation of fibroblasts and epithelialization, thus accelerating wound healing (Barrientos et al., 2008). We potentiate the usefulness of Ad-MSCs by transfecting with PDGF genes and upregulating PDGF expression by approximately 200-fold. In addition, VEGF, vascular related factor and COX-2 and IL-6, inflammatory factors, were slightly upregulated. Epidermis factors, KGF, EGF, and IGF-1, were not significantly expressed.

Regarding re-epithelialization, upon gross analysis at day 5, PDGF-MSCs groups showed the highest epithelialization rates among groups and significantly higher epithelialization rates than undifferentiated groups. At day 10, PDGF-CS and PDGF-MSCs groups tended to have higher rates than UCS and U-MSCs groups, although this was not significant. From the histopathological analysis, clear differences were identified. At day 5 for PDGF-MSCs groups and at day 10 for PDGF-CS, and PDGF-MSCs groups, there was significantly higher keratinocyte proliferation and a thicker neoepidermis observed than in undifferentiated groups. Rete ridges-like structures and skin appendages were frequently identified in the PDGF groups. Previous in vivo studies demonstrated that PDGF accelerated re-epithelialization in the wounds of many species with topical application, adenovirus-mediated expression, and gene transfer therapy (Liechty et al., 1999). The mechanism presumed was that PDGF upregulated the production of insulin-like growth factor-1 (IGF-1), which increased keratinocyte motility (Rabhi-Sabile et al., 1996) and PDGF activated and stimulated macrophages and fibroblasts to secrete keratinocyte-stimulating substances, like keratinocyte growth factor (KGF) (Pierce et al., 1991). Given that epidermis related factors, such as KGF, EGF, and IGF-1, were not significantly expressed in PDGF-CS and PDGF-MSCs, a great amount of PDGF expression might play a primary role in keratinocyte proliferation and re-epithelialization. One report assumed that the effect of PDGF on epithelialization was due to activated keratinocytes in wound margins reacting directly to PDGF (Pierce et al., 1991). In addition, intradermal injection of PDGF-B overexpression adenovirus around wounds presented significantly increased wound closure and re-epithelialization (Liechty et al., 1999).

A difference in epithelialization between the PDGF-CS and PDGF-MSCs was observed. PDGF-MSCs showed a significantly thicker neoepidermis at day 5 and progressively increased keratinocyte proliferation at day 10, but PDGF-CS presented a significance only at day 10. In addition, PDGF-MSCs indicated the most keratinocyte proliferation among the groups. Intradermal injection of PDGF-MSCs around the wound may induce large amounts of PDGF to work on keratinocytes of the epithelium while the PDGF-CS just contacts wound margins, in which small amounts of cells were delivered.

Wound contraction was related to locomotion of proliferating fibroblasts into wound beds and differentiation of fibroblasts into myofibroblasts (Darby et al., 1990). Myofibroblasts predominate within the wound and increase early wound closure (Richey et al., 1989). Fibroblasts make collagen to reinforce the wound as myofibroblasts contract (Stadelmann et al., 1998). MSCs increased contraction of the wound and reduced the healing time with significantly higher FGF levels in the wound (Uysal et al., 2014) and PDGF was known to play a role in contraction by enhancing the proliferation of fibroblasts, inducing the myofibroblast phenotype, and stimulating fibroblasts to construct collagen matrices (Barrientos et al., 2014). In the gross analysis, significant wound contraction was present in experimental groups, compared to control groups at day 10, although the PDGF groups showed no significant wound contraction compared to undifferentiated groups. Histologically, the width and depth of granulation tissue observed by H&E staining were more narrow and deeper, respectively, in experimental groups, while in control groups, the shape of granulation tissue was wide and shallow, which might suggest that experimental groups had more contraction of granulation tissues.

Among the experimental groups, the PDGF-CS groups showed the most granulation tissue formation and had higher histological scores than the UCS groups at day 10. In addition, collagens and activated fibroblasts were more abundant, dense and well organized in PDGF-CS groups than in UCS groups. PDGF stimulates mitogenicity and chemotaxis of fibroblasts, macrophages, and smooth muscle cells to wound areas (Heldin et al., 1999) and also increases macrophage-mediated tissue debridement and granulation tissue formation (Uutela et al., 2004). Although the exact mechanism has not been proven, the wound healing effect of exogenous PDGF has been demonstrated in other acute and chronic wound models (Gowda et al., 2015; Cheng et al., 2007). In the previous *in vivo* studies, PDGF was shown to improve the proliferation of fibroblasts and thus the production of ECM (Cheng et al., 2007; Lin et al., 2006). In addition, it stimulates fibroblasts to contract collagen matrices (Rhee et al., 2006) and enhances the granulation tissue formation (Cheng et al., 2007). As shown in the previously reported studies, presumably overexpressed PDGF seems to have an effect on the wound beds for granulation tissue formation and maturation.

The sheet groups presented both significant maturation of granulation tissue on day 5 and accelerated improvement in the quantity and quality of both upper and lower granulation tissue by day 10, while the cell groups only showed maturation of granulation tissues at day 10. The difference in granulation tissue response for cell sheets and cells may be attributable to the stem cell delivery system. Previous studies reported that the general approach for stem cell delivery has been the direct injection of single cell suspensions around the wound bed (Nie et al., 2011; Rodriguez et al., 2015); however, a few of the transplanted stem cells persist, migrate and participate in the wound bed (Suh et al., 2005). Also, a recent study showed that within the 2

weeks after intradermal injection around wounds, the number of MSCs was significantly decreased in the cutaneous wound bed (Wu et al., 2007). This was presumably because the residence time of MSCs in the wound bed was reduced (Wu et al., 2007) or the proper microenvironment was needed for MSCs survival and transdifferentiation (Yew et al., 2011). An innovative alternative to the limitation of cell injection is cell sheet engineering. Stem cell sheets are a scaffold-free approach in that cell-to-cell junctions are preserved via cell junction proteins and the cells became as a contiguous cell sheet along with their deposited extracellular matrix (Matsuda et al., 2007). Thereby, cell residence time, engraftment, and cell survival rates increased (Lin et al., 2013), thus overcoming one of the major problems with the injection of cell suspensions. One study reported that Ad-MSCs were detected in the wound bed at 21 days after applying cell sheets on the wound (McLaughlin and Marra, 2013). Long residences of MSCs in cell sheets could increase migration of fibroblasts and neo-vascularization in the wound bed.

In conclusion, PDGF-CS, UCS, PDGF-MSCs, and U-MSCs accelerated cutaneous wound healing. The PDGF-CS showed the most granulation tissue formation and maturation, and intradermal injection of PDGF-MSCs accelerated keratinocyte proliferation and epithelialization the most.

REFERENCES

Barrientos S, Brem H, Stojadinovic O, Tomic-Canic M. Clinical application of growth factors and cytokines in wound healing. Wound Repair Regen 2014; 22(5): 569-578.

Barrientos S, Stojadinovic O, Golinko MS, Brem H, Tomic-Canic M. Growth factors and cytokines in wound healing. Wound Repair Regen 2008; 16(5): 585-601.

Bohling MW, Henderson RA, Swaim SF, Kincaid SA, Wright JC. Cutaneous wound healing in the cat: A macroscopic description and comparison with cutaneous wound healing in the dog. Vet Surg 2004; 33(6): 579-587.

Cerqueira MT, Pirraco RP, Santos TC, Rodrigues DB, Frias AM, Martins AR, et al. Human adipose stem cells cell sheet constructs impact epidermal morphogenesis in full-thickness excisional wounds. Biomacromolecules 2013; 14(11): 3997-4008.

Cheng B, Liu HW, Fu XB, Sun TZ, Sheng ZY. Recombinant human platelet-derived growth factor enhanced dermal wound healing by a pathway involving ERK and c-fos in diabetic rats. J Dermatol Sc 2007; 45(3): 193-201.

Darby I, Skalli O, Gabbiani G. Alpha-smooth muscle actin is transiently expressed by myofibroblasts during experimental wound healing. Lab Invest 1990; 63(1): 21-29.

Embil JM, Papp K, Sibbald G, Tousignant J, Smiell JM, Wong B, et al. Recombinant human platelet-derived growth factor-BB (becaplermin) for healing chronic lower extremity diabetic ulcers: an open-label clinical evaluation of efficacy. Wound Repair Regen 2000; 8(3): 162-168.

Farghali, H.A, et al, Evaluation of subcutaneous infiltration of autologous platelet-rich plasma on skin wound healing in dogs. Biosci Rep 2017; BSR20160503.

Galiano RD, Tepper OM, Pelo CR, Bhatt KA, Callaghan M, Bastidas N, et al. Topical vascular endothelial growth factor accelerates diabetic wound healing through increased angiogenesis and by mobilizing and recruiting bone marrow-derived cells. Am J Pathol 2004; 164(6): 1935-1947.

Gowda S, Weinstein DA, Blalock TD, Gandhi K, Mast BA, Chin G, Schultz GS. Topical application of recombinant platelet-derived growth factor increases the rate of healing and the level of proteins that regulate this response. Int Wound J 2015; 12(5): 564-571.

Greenhalgh DG, Sprugel KH, Murray MJ, Ross R. PDGF and FGF stimulate wound healing in the genetically diabetic mouse. Am J Pathol. 1990; 136(6): 1235.

Heldin CH, Westermark B. Mechanism of action and in vivo role of platelet-derived growth factor. Physiol Rev 1999; 79(4): 1283-1316.

Hu MS, Maan ZN, Wu JC, Rennert RC, Hong WX, Lai TS, et al. Tissue engineering and regenerative repair in wound healing. Ann Biomed Eng 2014; 42(7): 1494-1507.

Isakson M, De Blacam C, Whelan D, McArdle A, Clover AJ. Mesenchymal stem cells and cutaneous wound healing: current evidence and future potential. Stem Cells Int 2015.

Jacobi J, Jang JJ, Sundram U, Dayoub H, Fajardo LF, Cooke JP. Nicotine accelerates angiogenesis and wound healing in genetically diabetic mice. Am J Pathol 2002; 161(1): 97-104.

Kern S, Eichler H, Stoeve J, Kluter H, Bieback K. Comparative analysis of mesenchymal stem cells from bone marrow, umbilical cord blood, or adipose tissue. Stem Cells 2006; 24(5): 1294-1301.

Kim CH, Lee JH, Won JH, Cho MK. Mesenchymal stem cells improve wound healing in vivo via early activation of matrix metalloproteinase-9 and vascular endothelial growth factor. J Korean Med Sci 2011; 26(6): 726-733.

Larouche D, Cuffley K, Paquet C. Tissue-engineered skin preserving the potential of epithelial cells to differentiate into hair after grafting. Tissue Eng Part A 2010; 17(5-6): 819-830.

Liechty KW, Nesbit M, Herlyn M, Radu A, Adzick NS, Crombleholme TM. Adenoviral-mediated overexpression of platelet-derived growth factor-B corrects ischemic impaired wound healing. J Invest Dermatol 1999; 113(3): 375-383.

Lin H, Chen B, Sun W, Zhao W, Zhao Y, Dai J. The effect of collagen-targeting platelet-derived growth factor on cellularization and vascularization of collagen scaffolds. Biomaterials 2006; 27(33): 5708-5714.

Lin YC, Grahovac T, Oh SJ, Ieraci M, Rubin JP, Marra KG. Evaluation of a multi-layer adipose-derived stem cell sheet in a full-thickness wound healing model. Acta Biomater 2013; 9(2): 5243-5250.

Livak KJ, Schmittgen TD. Analysis of relative gene expression data using real-time quantitative PCR and the 2−ΔΔCT method. Methods 2001; 25(4): 402-408.

Man LX, Park JC, Terry MJ. Lentiviral gene therapy with platelet-derived growth factor B sustains accelerated healing of diabetic wounds over time. Ann Plast Surg 2005; 55(1): 81-86.

Matsuda N, Shimizu T, Yamato M, Okano T. Tissue engineering based on cell sheet technology. Adv Mater 2007; 19(20): 3089-3099.

McLaughlin MM Marra KG. The use of adipose-derived stem cells as sheets for wound healing. Organogenesis 2013; 9(2): 79-81.

Nie C, Yang D, Xu J, Si Z, Jin X, Zhang J. Locally administered adipose-derived stem cells accelerate wound healing through differentiation and vasculogenesis. Cell Transplant 2011; 20(2): 205-216.

Pierce GF, Mustoe TA, Mustoe BW, Altrock TF, Deuel TF, Thomason A. Role of platelet-derived growth factor in wound healing. J Cell Biochem 1991; 45(4): 319-326.

Rabhi-Sabile S, Pidard D, Lawler J, Renesto P, Chignard M, Legrand C. Proteolysis of thrombospondin during cathepsin-G-induced platelet aggregation: functional role of the 165-kDa carboxy-terminal fragment. FEBS Lett 1996; 386(1): 82-86.

Rhee S, Grinnell F. P21-activated kinase 1: convergence point in PDGF-and LPA-stimulated collagen matrix contraction by human fibroblasts. J Cell Biol 2006; 172(3): 423-432.

Richey KJ, Engrav LH, Pavlin EG, Murray MJ, Gottlieb JR, Walkinshaw MD. Topical growth factors and wound contraction in the rat: Part I. Literature review and definition of the rat model. Ann Plast Surg 1989; 23(2): 159-165.

Robson MC, Payne WG, Garner WL, Biundo J, Giacalone VF, Cooper DM, Ouyang P. Integrating the results of phase IV (postmarketing) clinical trial with four previous trials reinforces the position that Regranex (becaplermin) gel 0.01%

is an effective adjunct to the treatment of diabetic foot ulcers. J Appl Res 2005; 5(1): 35-45.

Rodriguez J, Boucher F, Lequeux C, Josset-Lamaugarny A, Rouyer O, Ardisson O, et al. Intradermal injection of human adipose-derived stem cells accelerates skin wound healing in nude mice. Stem Cell Res Ther 2015; 6(1): 241.

Ryu HH, Lim JH, Byeon YE, Park JR, Seo MS, Lee YW, et al. Functional recovery and neural differentiation after transplantation of allogenic adipose-derived stem cells in a canine model of acute spinal cord injury. J Vet Sci 2009; 10(4): 273-284.

Stadelmann WK, Digenis AG, Tobin GR. Physiology and healing dynamics of chronic cutaneous wounds. Am J Surg 1998; 176(2): 26S-38S.

Suh W, Kim KL, Kim JM, Shin IS, Lee YS, Lee JY, et al. Transplantation of endothelial progenitor cells accelerates dermal wound healing with increased recruitment of monocytes/macrophages and neovascularization. Stem Cells 2005; 23(10): 1571-1578.

Uutela M, Wirzenius M, Paavonen K, Rajantie I, He Y, Karpanen T, et al. PDGF-D induces macrophage recruitment, increased interstitial pressure, and blood vessel maturation during angiogenesis. Blood 2004; 104(10): 3198-3204.

Uysal CA, Tobita M, Hyakusoku H, Mizuno H. The effect of bone-marrow-derived stem cells and adipose-derived stem cells on wound contraction and epithelization. Adv Wound Care 2014; 3(6): 405-413.

Wu Y, Chen L, Scott PG, Tredget EE. Mesenchymal stem cells enhance wound healing through differentiation and angiogenesis. Stem Cells 2007; 25(10): 2648-2659.

Yew TL, Hung YT, Li HY, Chen HW, Chen LL, Tsai KS, et al. Enhancement of wound healing by human multipotent stromal cell conditioned medium: tHE paracrine factors and p38 MAPK activation. Cell Transplant 2011; 20(5): 693-706.

국 문 초 록

혈소판유래성장인자 과발현 중간엽 줄기세포와 시트의 개 피부 창상 치유 효과

지도교수 권 오 경

김 남 열

서울대학교 대학원

수의학과 임상수의학 전공

지방 유래 중간엽 줄기세포는 창상 치유에 탁월한 잠재력을 가지고 있다. 또한 혈소판유래성장인자는 각 치유 단계에 중요한 역할을 하며, 정상 피부와 손상된 피부에 강력한 창상 치유 능력을 갖는다. 본 연구는 혈소판유래성장인자 과발현 중간엽줄기세포 (PDGF-MSCs)와 시트 (PDGF-CS), 미분화중간엽줄기세포 (U-MSCs)와 시트 (UCS)의 개 피부 창상 치유능력을 다각도로 비교하였다. 각 세포와 시트의 실험실적 비교에서, PDGF-MSCs와 PDGF-CS의 PDGF-B 분비가 200 배

상승하였음을 확인하였다. 개 피부창상모델 통한 육안적 비교에서, 모든 세포와 시트 적용군의 창상치유가 촉진되었으며 ($p < 0.05$), 조직학적 비교에서 특히 PDGF-MSCs 적용군에서 상피율의 상피세포증식에 유의적 증가가 확인되었다 ($p < 0.05$). 육아조직에서, PDGF-CS 와 UCS 적용군의 육아조직 상층 조직형성, 콜라겐 침착, 활성화 섬유아세포 형성이 PDGF-MSCs, U-MSCs 적용군 보다 유의적으로 높았다 ($p < 0.05$). 특히 PDGF-CS 적용군이 가장 많은 육아조직 형성과 성숙도를 보였다. 결론적으로 PDGF-MSCs는 상피형성에 가장 큰 촉진작용을 보였으며, PDGF-CS는 육아조직형성과 성숙에 가장 높은 작용을 보여줬다. 따라서 PDGF 과발현 세포와 시트는 개 창상치유에 효과적인 치료 방법으로 시도 될 수 있다.

주요어: 혈소판유래성장인자, 지방 유래 중간엽 줄기세포, 줄기세포 시트, 창상 치유, 개

학번: 2016-26345